Realizable Transmitters for Diffusive Molecular Communication

T. tom Dieck, L. Brand, S. Lotter, K. Castiglione, R. Schober, and M. Schäfer
Friedrich-Alexander-Universität Erlangen-Nürnberg

***Abstract*—Realistic transmitter (TX) models are crucial for the practical implementation of future molecular communication (MC) systems. However, most works in MC still rely on simplified and idealized TX models. In this abstract, we compare the idealized point TX to a novel realizable TX in a diffusive MC scenario with a fully absorbing receiver (RX). Moreover, we model the noise caused by the undesired leakage of the considered realizable TX and evaluate the performance of a threshold detector. Our results show a significant difference between both TX models, highlighting the importance of employing realistic TX models for the analysis of MC systems.**

I. Introduction

MC is a nature-inspired communication paradigm, where signalling molecules (SMs) are employed as information carriers. MC is envisioned to enable communication in environments where electromagnetic waves cannot be applied, e.g., inside the human body. However, most work in MC still relies on many simplifying assumptions, resulting in a lack of suitable models for practically realizable components, such as TXs and RXs, which are required for future applications. We analyze a diffusive MC system employing a chemically-realizable TX and compare it to the idealized point TX commonly adopted in the MC literature [1]. Moreover, we consider a realistic noise model, i.e., the uncontrollable leakage of SMs by the realizable TX, and compare it to a continuously emitting independent noise source, a model often adopted in the literature.

II. Communication System

The considered system is shown in Fig. 1. It comprises a nanoscale TX that can be controlled via a light-emitting diode (LED) [2], and a fully absorbing RX in a diffusive environment. The employed simulation method models the concentration of the SMs at the TX and then tracks the SMs released into the environment by particle-based simulation (PBS). We compare the number of received SMs obtained from PBS to analytical results for the point TX and the realizable TX (see [1] and [3]). On-off keying is employed as modulation scheme.

Realizable TX: We consider the realizable TX proposed in [2]. The TX consists of a synthetic polymer vesicle, loaded with SMs of type S. Transport proteins inserted into its membrane allow for the controlled release of S from the TX using the LED: Light-driven proton pumps (depicted in green in Fig. 1) create an H^+ gradient over the vesicle membrane, which is leveraged as energy source for the co-transport of S by so-called symporters (depicted in orange). For the transmission, we assume that the LED is turned on during bit "1" intervals and turned off during bit "0" intervals, respectively. In the simulations, we model the behavior of the TX according to the numerical baseline in [2]. Based on the obtained flux of S into the channel, for the PBS we generate individual S molecules randomly in each timestep with probability $i_{\mathrm{SM}}(t)N_{\mathrm{A}}\Delta t$, where $i_{\mathrm{SM}}(t)$, $N_{\mathrm{A}} = 6.022 \cdot 10^{23}\mathrm{mol}^{-1}$, and Δt are the flux of SMs from the vesicle in $\mathrm{mol\,s}^{-1}$, the Avogadro constant, and the duration of the timestep, respectively.

Point TX: As idealized model [1], we consider the release of SMs from a point TX. In this commonly applied model, the TX is an SM source without physical dimensions that is perfectly controllable and can release an arbitrary number of SMs instantaneously at the beginning of a bit "1" transmission. The number of SMs released from the point TX is chosen equal to the average number of released SMs of the realizable TX during one bit "1" transmission.

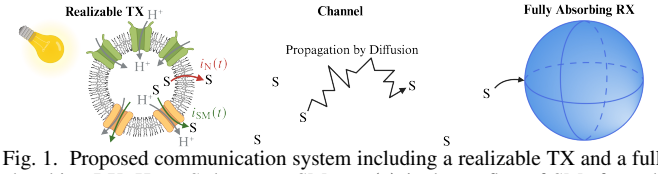

Fig. 1. Proposed communication system including a realizable TX and a fully absorbing RX. Here, S denotes a SM, $i_{\mathrm{SM}}(t)$ is the outflux of SMs from the TX, and $i_{\mathrm{N}}(t)$ is the leakage flux, i.e., noise (Created with BioRender.com).

Channel & RX: After their release from the TX, SMs diffuse freely in the environment. For the PBS, we model the behavior of individual S molecules by a random walk. We consider a fully-absorbing RX [1], which assumes that S molecules are instantaneously absorbed as they hit its surface. Additionally, the RX is able to count the number of S molecules that it has absorbed.

Noise Source: A common assumption in the MC literature is that an external noise source emits SMs at a constant rate causing interference at the RX. In practice, the TX itself possibly leaks SMs at non-desired times leading to noise [4]. For example, the vesicle membrane of the considered realizable TX is permeable to some molecules [5]. Therefore, depending on the choice of SMs, next to the desired active transport of SMs by transmembrane proteins, some SMs may passively *leak* from the vesicle by permeating through its membrane. As the leakage flux of SMs over the vesicle membrane ($i_{\mathrm{N}}(t)$ in Fig. 1) depends linearly on the concentration gradient across the membrane, this TX noise is inherently signal-dependent and decreases when less S is available inside the vesicle [2]. In our realistic TX model, we account for this TX noise and make a comparison with a point TX impaired by an independent noise source that continuously emits S at a constant rate equal to the initial leakage rate of the vesicle.

III. Single-Sample Detection Scheme

We consider a simple threshold detection scheme derived for the fully absorbing RX and the point TX to find an estimate $\hat{s}[k]$ for the k-th transmitted symbol $s[k] \in \{0, 1\}$. For the point TX, it is easy to obtain the optimal threshold when neglecting inter-symbol interference (ISI). Applying the derived decision rule also for the realizable TX, reveals whether a standard thresholding scheme derived for an idealized scenario is suitable for reliable detection in a more realistic MC system, see Section IV. We assume that the RX samples once at the end of each bit interval. For an absorbing RX, it is useful to perform threshold detection based on the difference between the current sample $r[k] = R(T_{\mathrm{b}}+kT_{\mathrm{b}})$ and the previous sample $r[k-1]$, where $R(t)$ and T_{b} are the accumulated received signal at time t and the bit duration, respectively. We decide for $\hat{s}[k] = 1$ iff $r[k] - r[k-1] \geq \xi$, where ξ denotes the decision threshold. For the derivation of the optimal threshold ξ^* for the point TX, we minimize the probability of error, P_{e}, i.e., $\xi^* = \arg\min_{\xi} P_{\mathrm{e}}$, where we neglect the impact of ISI and

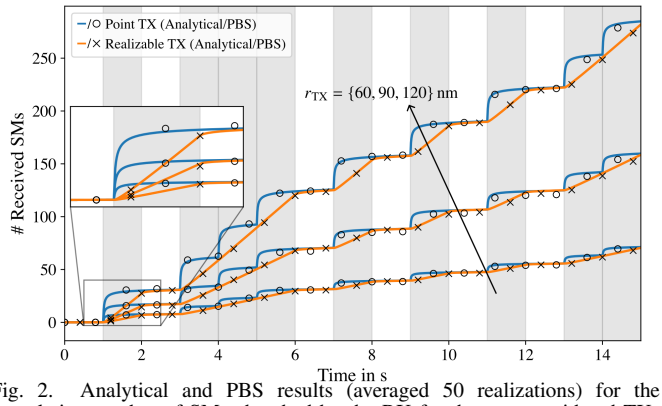

Fig. 2. Analytical and PBS results (averaged 50 realizations) for the cumulative number of SMs absorbed by the RX for the two considered TXs and three different TX radii, r_{TX}. Gray shading indicates bit "1".

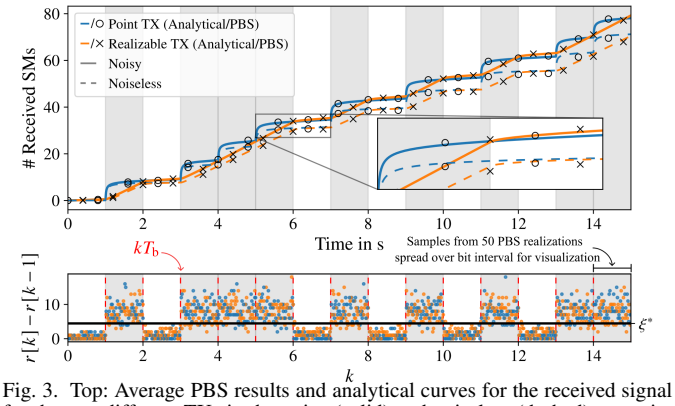

Fig. 3. Top: Average PBS results and analytical curves for the received signal for the two different TXs in the noisy (solid) and noiseless (dashed) scenario, respectively. Bottom: Detection samples $r[k] - r[k-1]$ for each of the 50 PBS realizations for the point TX (blue) and the realizable TX (orange) and threshold ξ^* (black line).

assume that the number of received noise molecules and SMs can be modelled by a Poisson distribution. Thus, we obtain $\xi^* = \bar{n}_{SM} - \ln((\bar{n}_{SM} - \bar{n}_N)/\bar{n}_N)$ for the point TX, where $\bar{n}_{SM}$ and $\bar{n}_N$ are the average numbers of received SMs during a bit "1" transmission and received noise molecules, respectively [6].

IV. Simulation Results

Received Signal: Fig. 2 shows the received signal for the noiseless transmission of 15 random bits by the realizable TX (red curves) and the idealized point TX (blue curves) obtained based on analytical expressions[1] (solid curves) and PBS (markers), respectively, for different TX radii. The gray shading indicates bit "1" transmissions, i.e., times during which the LED is turned on. The received signals clearly differ for the two considered TX types. These deviations are mainly caused by the different release mechanisms of the TXs: the point TX releases SMs instantaneously causing a fast increase in the number of received SMs at the beginning of a bit "1" interval, while the realizable TX causes continuous SM release leading to a steady increase of SMs during the entire bit interval. This continuous release also leads to some incline during bit "0" intervals following a bit "1" for the realizable TX (see inlet). These differences in the received signal must be considered when designing suitable modulation and detection schemes. Moreover, Fig. 2 shows that increasing the diameter of the realizable TX results in a faster release of SMs. This results from the different number of inserted transport proteins whose density in the vesicle membrane is assumed constant [2].

Noisy Transmission: The top panel of Fig. 3 shows the received signal in the noisy scenario (solid lines) in comparison to the noiseless case (dashed lines). Generally, the additional release of noise molecules leads to higher molecule counts at the RX for both the point TX and the realizable TX. The impact of the noise molecules can be observed best during bit "0" transmissions, where the slope of the received signal is larger in the noisy scenario. The bottom panel of Fig. 3 shows the detection samples for each realization of the PBS for the point TX (blue) and the realizable TX (red)[2], as well as the optimal threshold ξ^* for the point TX (black line in the bottom plot of Fig. 3, derived in Section III). The average number of detection errors caused for the 50 realizations of the PBS of 15 random bit transmissions is 0.6 for the point TX and 1.04 for the realizable TX, where for both cases the detection rule derived for the point TX was applied. The error count is higher for the realizable TX (as is also expected from the bottom plot of Fig. 3), as the threshold was derived for the point TX and might not be optimal for the realizable TX. Furthermore, SMs released at the end of a bit interval by the realizable TX have a higher chance of not being detected within the current symbol interval. Consequently, the consideration of realistic release mechanisms is vital for deriving optimal detection schemes. Robust detection is pivotal for ensuring reliable communication in future MC systems.

[1]The analytical results reflect the propagation of SMs through the channel and their absorption at the RX for a given transmit signal. Due to space constraints, we do not provide the derivations here.

[2]Note that while for all 50 realizations of the PBS, the samples are taken at the sampling instance kT_b, the samples are plotted uniformly across each bit interval for better distinguishability.

V. Conclusion and Future Work

In this abstract, we investigated the importance of realistic TX and noise models for the analysis and design of MC systems. Our results showed a significant difference between a realistic TX model and the commonly applied point TX model. This highlights the importance of carefully modeling the release kinetics of realizable TXs to adequately predict the received signal in practically relevant MC systems. We compare the performances of the two TXs for a simple differential threshold detector which was optimized for the point TX, showing that the realizable TX generally performs worse. In future work, we plan to analyze whether the performance degradation is caused by the application of the suboptimal threshold or if the type of the release itself inherently limits performance.

References

[1] V. Jamali *et al.*, "Channel modeling for diffusive molecular communication—A tutorial review," *Proc. IEEE*, vol. 107, pp. 1256–301, Jul. 2019.

[2] T. tom Dieck *et al.*, "Nanoscale transmitters employing cooperative transmembrane transport proteins for molecular communication," in *Proc. 11th ACM Int. Conf. Nanosc. Comp. Commun.* ACM, Oct. 2024, pp. 14–20.

[3] X. Huang, Y. Fang, A. Noel, and N. Yang, "Membrane fusion-based transmitter design for static and diffusive mobile molecular communication systems," *IEEE Trans. Commun.*, vol. 70, pp. 132–148, Jan. 2022.

[4] A. Noel, K. C. Cheung, and R. Schober, "A unifying model for external noise sources and ISI in diffusive molecular communication," *IEEE J. Sel. Areas Commun.*, vol. 32, pp. 2330–2343, Dec. 2014.

[5] E. Rideau *et al.*, "Liposomes and polymersomes: A comparative review towards cell mimicking," *Chem. Soc. Rev.*, vol. 47, Sep. 2018.

[6] R. Mosayebi *et al.*, "Receivers for diffusion-based molecular communication: Exploiting memory and sampling rate," *IEEE J. Sel. Areas Commun.*, vol. 32, pp. 2368–2380, Dec. 2014.